Int. J. Solids Structures Vol. 30, No. 23, pp. 3281–3301, 1993
Printed in Great Britain

0020–7683/93 $6.00+ .00

METHOD OF DOMAIN DECOMPOSITION IN VIBRATIONS OF MIXED EDGE ANISOTROPIC PLATES

K. M. LIEW, K. C. HUNG and M. K. LIM
Dynamics and Vibration Centre, School of Mechanical and Production Engineering,
Nanyang Technological University, Nanyang Avenue, Singapore 2263

(*Received* 27 *July* 1992; *in revised form* 14 *June* 1993)

Abstract—This paper presents the first known study on the flexural vibration of anisotropic plates with mixed discontinuous periphery boundaries. A newly developed domain decomposition method is used in the analysis to derive the governing eigenvalue equation. In the solution process, the complex plate domain is decomposed into appropriate subdomains. The displacement functions of each subdomain are represented by sets of orthogonally generated polynomials that satisfy the essential geometric boundary conditions. From the compatibility requirements at the interconnecting boundaries, sets of continuity matrices are computed. These matrices are used to couple the respective eigenvectors of the adjacent subdomains. The stiffness and mass matrices of each subdomain after being pre- and post-multiplied by the corresponding continuity matrix, are assembled to form the global stiffness and mass matrices of the anisotropic plate. Convergence and comparison studies have been carried out on selected cases to establish the rate of convergence and degree of accuracy of the present formulation. A comprehensive range of frequency parameters and deflection mode shapes of anisotropic plates with different mixed edge configurations are obtained using the proposed method. The effects of fiber orientation and the partial mixed ratio on the vibrational response of these plates have been investigated in detail.

1. INTRODUCTION

The superior property of composite materials has widened their applications in many branches of engineering. Increasingly, structural elements in civil, mechanical, marine and aeronautical applications are made of composites to reduce their weight and in addition, to maximize their strength. The widespread use of these advanced materials has rendered the understanding of their dynamic behaviors of high practical importance.

The transverse vibration of an anisotropic plate is governed by the following partial differential equation:

$$D_{11}\frac{\partial^4 w}{\partial x^4}+4D_{16}\frac{\partial^4 w}{\partial x^3\,\partial y}+2(D_{12}+2D_{66})\frac{\partial^4 w}{\partial x^2\,\partial y^2}+4D_{26}\frac{\partial^4 w}{\partial x\,\partial y^3}+D_{22}\frac{\partial^4 w}{\partial y^4}-\rho h\frac{\partial^2 w}{\partial t^2}=0. \tag{1}$$

The presence of odd derivatives in the terms containing D_{16} and D_{26} prevents the equation from yielding exact solutions. Numerical approximation has been commonly resorted to for solutions. Ashton (1969) used the Ritz method to study the vibration response of completely free square plates. The effect of anisotropy on the natural frequency and mode shapes has been investigated. Bert (1977a,b) introduced a simple reduction method to study the vibration of orthotropic plates with various planforms and boundary conditions. Chelladurai *et al.* (1984) used a high precision triangular finite element to study the free vibration of rectangular orthotropic plates with varying fiber orientation. Malhotra *et al.* (1988) further examined the influence of fiber orientation on the flexural vibration of orthotropic plates by both the finite element and the Rayleigh–Ritz methods. A solution method using the two-dimensional orthogonal polynomial functions in the Rayleigh–Ritz procedure (Liew *et al.*, 1989) has also been proposed to study the vibration of triangular anisotropic plates. Other approximate methods based on the Galerkin procedure (Mohan and Kingsbury, 1971) and the classical Fourier analysis (Whitney, 1971) have also been applied to the vibration analysis of these composites.

From the brief review of the literature, it is found that the approximate methods for the vibrational analysis of plates with skew orthotropy subjected to simple boundary

conditions are well documented. No literature was found, however, for the anisotropic plates with mixed edge boundary conditions. Solution methods for this class of plates made of isotropic material abound. Both analytical methods (Ota and Hamada, 1963; Keer and Stahl, 1972; Narita, 1981; Gorman, 1984) and discretization methods (Venkateswara *et al.*, 1973; Fan and Cheung, 1984; Mizusawa and Leonard, 1990; Liew *et al.*, 1993a) have been developed for the vibrational modeling of plates with mixed discontinuous periphery boundaries. In a very recent study, a domain decomposition method (Liew *et al.*, 1993b) has been developed for the analysis of isotropic plates with mixed periphery boundaries. Natural frequencies and mode shapes of a wide class of mixed edge plates have been presented. The success implementation of the domain decomposition method (DDM) to the analysis of isotropic mixed edge plates has further prompted the present work of extending its application to the analysis of fiber-reinforced anisotropic plates with mixed discontinuous periphery boundaries.

In this paper, the detailed formulation of the domain decomposition method for the vibrational modeling of anisotropic plates with mixed edge boundary conditions is discussed. In the solution process, the complex plate geometry is decomposed into appropriate simple geometric subdomains. The admissible functions for each subdomain are chosen from a set of orthogonal polynomials that satisfy the essential boundary conditions of the subdomain. The continuity matrices resulting from the geometric compatibility requirement between the subdomains are used to couple the eigenvectors of adjacent subdomains. The stiffness and mass matrices of each subdomain after being pre- and post-multiplied by the respective continuity matrices are assembled to form the global stiffness and mass matrices of the anisotropic plate. The eigenvalue equation of the plate with mixed edge conditions is derived subsequently from the minimization of the global energy functional in the Ritz procedure.

The primary objectives of the present work are (a) to provide the first known natural frequencies and mode shapes for an important class of fiber-reinforced anisotropic plates with partial mixed periphery boundaries, and (b) to investigate the effects of the fiber orientation and partial mixed ratio on the vibrational response of these plates. The results presented in this study are believed to be useful to the practicing engineers working in this field.

2. METHOD OF ANALYSIS

Consider the free flexural vibration of a fiber-reinforced anisotropic plate with partial discontinuous edges along the periphery boundaries as shown in Fig. 1. The edges of the anisotropic plate lying in the x–y plane are bounded by $-a/2 \leqslant x \leqslant a/2$ and $-b/2 \leqslant y \leqslant b/2$.

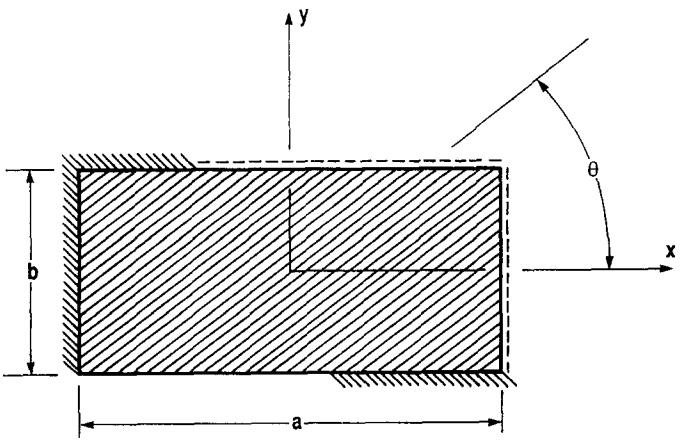

Fig. 1. Geometry of a fiber-reinforced anisotropic plate with partial mixed discontinuous periphery boundaries.

2.1. *The method of domain decomposition*

To establish the governing eigenvalue equation for this problem, the complex plate domain is decomposed into small subdomains with simple boundary conditions as shown in Fig. 2. The displacement function of each subdomain is chosen to satisfy the corresponding essential boundary conditions:

$$W^{\{1\}}(x, y) = \sum_{i=1}^{I} \sum_{j=1}^{J} c_{ij}^{\{1\}} \phi_i^{\{1\}}(x) \psi_j^{\{1\}}(y) \tag{2}$$

and

$$W^{\{\varepsilon\}}(x, y) = \sum_{i=1}^{I} \sum_{j=1}^{J} c_{ij}^{\{\varepsilon\}} \phi_i^{\{\varepsilon\}}(x) \psi_j^{\{\varepsilon\}}(y), \tag{3}$$

where $\varepsilon = 2, 3, \ldots, M_e$ represents the subdomain indices and M_e is the total number of subdomains. Depending on the relative location of each subdomain, the respective displacement function will share an identically generated set of admissible functions either in the x- or y-direction, i.e.

$$\phi_i^{\{\varepsilon\}}(x) = \phi_i^{\{\varepsilon-1\}}(x); \quad i = 1, 2, 3, \ldots, I \tag{4a}$$

or

$$\psi_j^{\{\varepsilon\}}(y) = \psi_j^{\{\varepsilon-1\}}(y); \quad j = 1, 2, 3, \ldots, J. \tag{4b}$$

To satisfy the compatibility requirement at the interconnecting boundaries, the continuities in deflection, slope and higher derivatives of the admissible function are imposed concurrently. Evenly distributed quadrature segments are defined along the interconnecting boundaries for the enforcement of these continuity conditions. The method of Subdomain Weighted Residual (Grandin, 1986) is applied at these quadrature segments with a weighting function of unity:

$$\int_{s_i} E(s)\, \mathrm{d}s = 0; \quad i = 1, 2, 3, \ldots, n, \tag{5}$$

where $E(s)$ is the error function representing the relative difference in displacement, slope and higher order derivatives between the adjacent subdomains. This function is minimized simultaneously over separate regions of the integral. In explicit form, this implies:

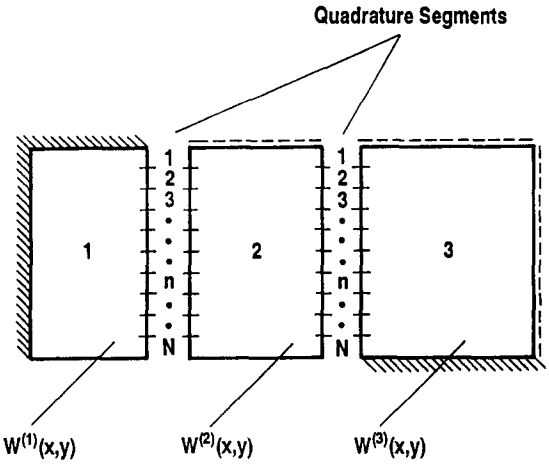

Fig. 2. Decomposition of plate domain and the distribution of quadrature segments.

$$\int_{s_{n-1}}^{s_n} (W^{\{\varepsilon\}} - W^{\{\varepsilon-1\}})\,ds = 0, \tag{6a}$$

$$\int_{s_{n-1}}^{s_n} \left(\frac{\partial W^{\{\varepsilon\}}}{\partial s} - \frac{\partial W^{\{\varepsilon-1\}}}{\partial s}\right) ds = 0, \tag{6b}$$

$$\vdots$$

$$\int_{s_{n-1}}^{s_n} \left(\frac{\partial^r W^{\{\varepsilon\}}}{\partial s^r} - \frac{\partial^r W^{\{\varepsilon-1\}}}{\partial s^r}\right) ds = 0, \tag{6c}$$

where $n = 1, 2, 3, \ldots, N$; $\varepsilon = 2, 3, \ldots, M_e$; $r = 1, 2, 3, \ldots, J-1$ and $s = x$ or y depending on the direction of continuities to be enforced. The deflection functions, W, of each subdomain have been defined in eqns (2) and (3).

A set of continuity matrices that coupled the eigenvectors C_{ij} of the adjacent subdomains can be obtained directly from the above simultaneous equations. The derivation process is illustrated for subdomains 1 and 2. These two subdomains share an identical set of admissible functions in the x-direction, i.e.

$$\phi_i^{\{1\}}(x) = \phi_i^{\{2\}}(x); \quad \text{for} \quad i = 1, 2, \ldots, I. \tag{7}$$

From eqns (6) and (7), the following set of simultaneous equations is obtained;

$$\mathscr{Z}_1\phi_1^{\{1\}} + \mathscr{Z}_2\phi_2^{\{1\}} + \cdots + \mathscr{Z}_i\phi_i^{\{1\}} + \cdots + \mathscr{Z}_I\phi_I^{\{1\}} = 0, \tag{8a}$$

$$\mathscr{Z}_1\frac{\partial\phi_1^{\{1\}}}{\partial x} + \mathscr{Z}_2\frac{\partial\phi_2^{\{1\}}}{\partial x} + \cdots + \mathscr{Z}_i\frac{\partial\phi_i^{\{1\}}}{\partial x} + \cdots + \mathscr{Z}_I\frac{\partial\phi_I^{\{1\}}}{\partial x} = 0, \tag{8b}$$

$$\vdots$$

$$\mathscr{Z}_1\frac{\partial^r\phi_1^{\{1\}}}{\partial x^r} + \mathscr{Z}_2\frac{\partial^r\phi_2^{\{1\}}}{\partial x^r} + \cdots + \mathscr{Z}_i\frac{\partial^r\phi_i^{\{1\}}}{\partial x^r} + \cdots + \mathscr{Z}_I\frac{\partial^r\phi_I^{\{1\}}}{\partial x^r} = 0, \tag{8c}$$

where

$$\mathscr{Z}_i = \left[\sum_{j=1}^{J} c_{ij}^{\{1\}} \int \psi_j^{\{1\}}(y)\,dy - \sum_{j=1}^{J} c_{ij}^{\{2\}} \int \psi_j^{\{2\}}(y)\,dy\right]. \tag{9}$$

The integration in eqn (9) is performed over the respective quadrature segments distributed along the interconnecting boundary. To satisfy eqns (8) simultaneously, all the terms in $\mathscr{Z}_i$ must be vanished identically;

$$\mathscr{Z}_1 = \mathscr{Z}_2 = \cdots = \mathscr{Z}_I = 0. \tag{10}$$

From eqn (10), the continuity matrix that coupled the eigenvectors of subdomains 1 and 2 is obtained:

$$\{c^{\{2\}}\} = [P^{\{2\}}]\{c^{\{1\}}\}. \tag{11}$$

The continuity matrix has the following form:

$$[P^{\{2\}}] = \begin{bmatrix} [p] & & & & \\ & [p] & & & \\ & & [p] & & \\ & & & \ddots & \\ & & & & [p] \end{bmatrix} \tag{12}$$

and the submatrix $[p]$ is given by,

$$[p] = [q^{\{2\}}]^{-1}[q^{\{1\}}], \tag{13}$$

where $[q^{\{\varepsilon\}}]$, $\varepsilon = 1, 2$, is a fully populated matrix of the form:

$$[q^{\{\varepsilon\}}] = \begin{bmatrix} q_{11}^{\{\varepsilon\}} q_{12}^{\{\varepsilon\}} q_{13}^{\{\varepsilon\}} & \cdots & q_{1j}^{\{\varepsilon\}} & \cdots & q_{1J}^{\{\varepsilon\}} \\ q_{21}^{\{\varepsilon\}} q_{22}^{\{\varepsilon\}} q_{23}^{\{\varepsilon\}} & \cdots & q_{2j}^{\{\varepsilon\}} & \cdots & q_{2J}^{\{\varepsilon\}} \\ \vdots & & \vdots & & \vdots \\ q_{n1}^{\{\varepsilon\}} q_{n2}^{\{\varepsilon\}} q_{n3}^{\{\varepsilon\}} & \cdots & q_{nj}^{\{\varepsilon\}} & \cdots & q_{nJ}^{\{\varepsilon\}} \\ \vdots & & \vdots & & \vdots \\ q_{N1}^{\{\varepsilon\}} q_{N2}^{\{\varepsilon\}} q_{N3}^{\{\varepsilon\}} & \cdots & q_{Nj}^{\{\varepsilon\}} & \cdots & q_{NJ}^{\{\varepsilon\}} \end{bmatrix}. \tag{14}$$

The elements of the matrix, $q_{nj}^{\{\varepsilon\}}$ are computed from the following integration:

$$q_{nj}^{\{\varepsilon\}} = \int_{x_{n-1}}^{x_n} \phi_i^{\{\varepsilon\}}(x)\,\mathrm{d}x \tag{15a}$$

or

$$q_{nj}^{\{\varepsilon\}} = \int_{y_{n-1}}^{y_n} \psi_j^{\{\varepsilon\}}(y)\,\mathrm{d}y. \tag{15b}$$

The subscript n in the above expression represents the indices of the quadrature segments whereas the subscripts i, j represent the indices of the polynomial functions. The derivation of the continuity matrix described above can be easily generalized to three or more subdomains.

2.2. *Orthogonal polynomial functions*

In the present study, the admissible functions, $\phi_i(x)$ and $\psi_j(y)$, are sets of orthogonally generated polynomial functions. These functions are intrinsically the products of (1) a basic function, and (2) an orthogonal polynomials space. The basic functions, $\phi_1(x)$ and $\psi_1(y)$ are chosen to satisfy at least the geometric boundary conditions of the subdomain. These functions are defined as follows:

$$\phi_1(x) = (x-a/2)^{\Omega_1}(x+a/2)^{\Omega_2}, \tag{16a}$$

$$\psi_1(y) = (y-b/2)^{\Omega_1}(y+b/2)^{\Omega_2}. \tag{16b}$$

The value of Ω_i $(i = 1, 2)$, depending on the boundary conditions of the supporting edge takes on:

$$\begin{cases} \Omega_i = 0 & \text{if } i\text{th edge is free;} \quad (17a) \\ \Omega_i = 1 & \text{if } i\text{th edge is simply supported;} \quad (17b) \\ \Omega_i = 2 & \text{if } i\text{th edge is clamped.} \quad (17c) \end{cases}$$

The higher order polynomials, $\phi_i(x)$ [or $\psi_j(y)$] are generated using the Gram–Schmidt orthogonalization process (Chihara, 1978):

$$\phi_{k+1}(x) = \{x-\Xi_k\}\phi_k(x)-\Theta_k\phi_{k-1}(x); \quad k = 1,2,3,\ldots, \tag{18}$$

where

$$\Xi_k = \frac{\int_{-a/2}^{a/2} x\phi_k^2(x)\,dx}{\int_{-a/2}^{a/2} \phi_k^2(x)\,dx} \tag{19a}$$

and

$$\Theta_k = \frac{\int_{-a/2}^{a/2} \phi_k^2(x)\,dx}{\int_{-a/2}^{a/2} \phi_{k-1}^2(x)\,dx}. \tag{19b}$$

The polynomial $\phi_0(x)$ is defined as zero and the sets of polynomials generated satisfy the orthogonality condition:

$$\int_{-a/2}^{a/2} \phi_i(x)\phi_j(x)\,dx = n_{ij}\delta_{ij}, \tag{20}$$

where δ_{ij} is the Kronecker delta and the value of n_{ij} depends on the normalization used. Orthogonal functions in the y-direction can be generated in a similar manner except that the limits of integration become $-b/2$ to $b/2$.

2.3. *Eigenvalue equation*

The stress–strain relations for the general anisotropic plate under plane stress is given by:

$$\begin{Bmatrix}\sigma_x\\ \sigma_y\\ \tau_{xy}\end{Bmatrix} = \begin{bmatrix}D_{11} & D_{12} & D_{16}\\ D_{12} & D_{22} & D_{26}\\ D_{16} & D_{26} & D_{66}\end{bmatrix}\begin{Bmatrix}\varepsilon_x\\ \varepsilon_y\\ \gamma_{xy}\end{Bmatrix}, \tag{21}$$

where D_{ij} are the bending stiffnesses of the anisotropic plate which are given by (Vinson and Sierakowski, 1986):

$$D_{11} = Q_{11}c^4+2(Q_{12}+2Q_{66})s^2c^2+Q_{22}s^4, \tag{22a}$$

$$D_{12} = (Q_{11}+Q_{22}-4Q_{66})s^2c^2+Q_{12}(s^4+c^4), \tag{22b}$$

$$D_{22} = Q_{11}s^4+2(Q_{12}+2Q_{66})s^2c^2+Q_{22}c^4, \tag{22c}$$

$$D_{16} = (Q_{11}-Q_{12}-2Q_{66})c^3s+(Q_{12}-Q_{22}+2Q_{66})s^3c, \tag{22d}$$

$$D_{26} = (Q_{11}-Q_{12}-2Q_{66})s^3c+(Q_{12}-Q_{22}+2Q_{66})c^3s, \tag{22e}$$

$$D_{66} = (Q_{11}+Q_{22}-2Q_{12}-2Q_{66})s^2c^2+Q_{66}(s^4+c^4), \tag{22f}$$

in which $s = \sin\theta$, $c = \cos\theta$ and

$$Q_{11} = \frac{E_1}{1-\nu_{12}\nu_{21}}, \quad Q_{12} = \frac{\nu_{12}E_2}{1-\nu_{12}\nu_{21}}, \tag{23a, b}$$

$$Q_{22} = \frac{E_2}{1-\nu_{12}\nu_{21}}, \quad Q_{66} = G_{12}, \quad \nu_{21}E_1 = \nu_{12}E_2. \tag{23c, d, e}$$

E_1 and E_2 are the Young's moduli parallel and perpendicular to the fibers respectively; ν_{12} and ν_{21} are the corresponding Poisson's ratios.

Let the strain energy $U^{\{\varepsilon\}}$ and kinetic energy $T^{\{\varepsilon\}}$ for a rectangular subdomain $\{\varepsilon\}$ be expressed in terms of the eigenvectors, c_{ij} of subdomain $\{1\}$:

$$U^{\{\varepsilon\}} = \int_A \{c^{\{1\}}\}^T [\bar{K}^{\{\varepsilon\}}] \{c^{\{1\}}\} \, dA \tag{24}$$

and

$$T^{\{\varepsilon\}} = \int_A \{c^{\{1\}}\}^T [\bar{M}^{\{\varepsilon\}}] \{c^{\{1\}}\} \, dA. \tag{25}$$

The transformed stiffness matrix $[\bar{K}^{\{\varepsilon\}}]$ and mass matrix $[\bar{M}^{\{\varepsilon\}}]$ for subdomain $\{\varepsilon\}$ are derived from the continuity matrix $[P^{\{\varepsilon\}}]$ of eqn (12):

$$[\bar{K}^{\{\varepsilon\}}] = [Q^{\{\varepsilon\}}]^T [K^{\{\varepsilon\}}] [Q^{\{\varepsilon\}}] \tag{26}$$

and

$$[\bar{M}^{\{\varepsilon\}}] = [Q^{\{\varepsilon\}}]^T [M^{\{\varepsilon\}}] [Q^{\{\varepsilon\}}], \tag{27}$$

where

$$\{Q^{\{\varepsilon\}}] = \prod_{s=2}^{\varepsilon} [P^{\{s\}}]. \tag{28}$$

For the fiber-reinforced anisotropic plate the elements of the matrices $[K^{\{\varepsilon\}}]$ and $[M^{\{\varepsilon\}}]$ are expressed as

$$K_{mnij} = \frac{1}{D_0} \{D_{11} E_{mi}^{22} F_{nj}^{00} + D_{22} E_{mi}^{00} F_{nj}^{22} + (E_{mi}^{02} F_{nj}^{20} + E_{mi}^{20} F_{nj}^{02}) + 2D_{16}(E_{mi}^{21} F_{nj}^{01} + E_{mi}^{12} F_{nj}^{10}) + 2D_{26}(E_{mi}^{01} F_{nj}^{21} + E_{mi}^{10} F_{nj}^{12}) + 4D_{66} E_{mi}^{11} F_{nj}^{11}\} \tag{29}$$

and

$$M_{mnij} = E_{mi}^{00} F_{nj}^{00}, \tag{30}$$

where $m, i = 1, 2, 3, \ldots, I$ and $n, j = 1, 2, 3, \ldots, J$.

$$E_{mi}^{rs} = \int \left[\frac{d^r \phi_m(x)}{dx^r} \frac{d^s \phi_i(x)}{dx^s} \right] dx \tag{31}$$

and

$$F_{nj}^{rs} = \int \left[\frac{d^r \psi_n(y)}{dy^r} \frac{d^s \psi_j(y)}{dy^s} \right] dy, \tag{32}$$

in which $r, s = 0, 1, 2$. The limits of integration in eqns (31) and (32) depend on the x- and y-dimensions of the individual subdomain.

The respective strain and kinetic energies of each subdomain are assembled to form the total strain energy, $\mathbb{U}$, and total kinetic energy, $\mathbb{T}$, of the entire plate, i.e.

$$\mathbb{U} = U^{\{1\}} + \sum_{\varepsilon=2}^{M_e} U^{\{\varepsilon\}} \tag{33}$$

and

$$\mathbb{T} = T^{\{1\}} + \sum_{\varepsilon=2}^{M_e} T^{\{\varepsilon\}}. \tag{34}$$

Substituting the total strain and kinetic energy expressions given by eqns (33) and (34) into the total energy functional,

$$\mathbb{F} = \mathbb{U} - \mathbb{T} \tag{35}$$

and applying the Ritz method of minimization,

$$\frac{\partial \mathbb{F}}{\partial c_{ij}^{\{1\}}} = 0; \quad i, j = 1, 2, 3, \ldots \tag{36}$$

leads to the governing eigenvalue equation for the entire plate domain:

$$([\mathbb{K}] - \lambda^2[\mathbb{M}])\{c^{\{1\}}\} = \{0\}. \tag{37}$$

The elements of the final stiffness matrix, $[\mathbb{K}]$, and the final mass matrix, $[\mathbb{M}]$, are given by

$$[\mathbb{K}] = [K^{\{1\}}] + \sum_{\varepsilon=2}^{M_e} [\bar{K}^{\{\varepsilon\}}] \tag{38}$$

and

$$[\mathbb{M}] = [M^{\{1\}}] + \sum_{\varepsilon=2}^{M_e} [\bar{M}^{\{\varepsilon\}}]. \tag{39}$$

The natural frequencies and coefficients for the deflection mode shapes [eqns (2) and (3)] are obtained by solving the governing eigenvalue equation defined by eqn (37).

From the above numerical formulation, it should be noted that the important merit of the present method is that, regardless of the number of subdomains involved, the assembling process of the global stiffness and mass matrices does not increase the determinant size of the final eigenvalue equation. Consequently, computational time and storage space can be reduced drastically. Recently, Yuan and Dickinson (1992) have proposed a new solution method for the vibration of rectangular plate systems. The compatibility conditions between adjacent plates are satisfied by imposing artificial springs along the interconnecting boundaries. Interesting and accurate vibration results for different complex plate problems have been presented. However, the determinant size of the problem in this approach, unlike the decomposition method, grows with the number of constitutive rectangular elements used in the formulation.

3. PROBLEM FORMULATION

The domain decomposition method developed in the preceding section is applied to solve the flexural vibration problems of selected mixed edge plate configurations. The

geometries and dimensions of these practical examples are depicted in Figs 3(a–d). The mixed edge ratio, β, is defined as c/a for all cases considered.

3.1. *A simply-supported plate partially clamped at two opposite edges*

The first case considered in the present study is a simply-supported plate, as shown in Fig. 3(a), partially clamped at the end of two opposing edges at $y = \pm b/2$. The domain is divided along the clamped portions into two subdomains. The deflection functions in the x-direction of each subdomain are identically generated to satisfy the simple support conditions at $x = \pm a/2$:

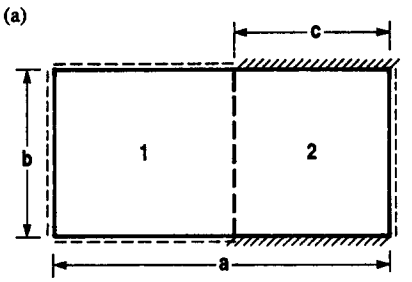

Fig. 3(a). A simply-supported plate partially clamped along the ends of two opposite edges.

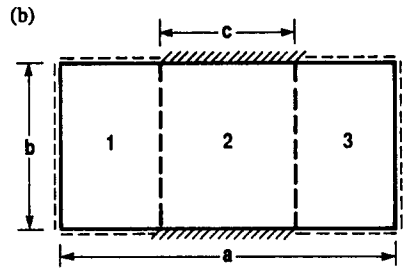

Fig. 3(b). A simply-supported plate partially clamped along the centers of two opposite edges.

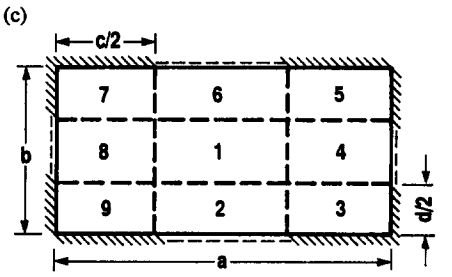

Fig. 3(c). A simply-supported plate partially clamped symmetrically from four corners.

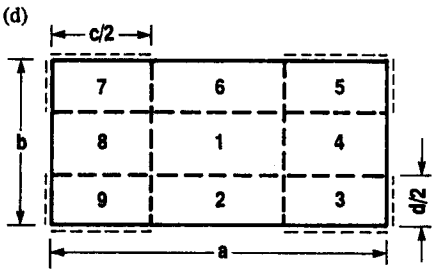

Fig. 3(d). A completely free plate partially simply-supported symmetrically from four corners.

$$W(\pm a/2, y) = \frac{\partial^2 W(\pm a/2, y)}{\partial x^2} = 0. \tag{40}$$

To account for the discontinuity boundaries at $y = \pm b/2$, different sets of functions are generated in the y-direction for various subdomains. For subdomain 1, the simple support conditions are to be satisfied:

$$W(x, \pm b/2) = \frac{\partial^2 W(x, \pm b/2)}{\partial y^2} = 0. \tag{41}$$

The relevant clamped boundary constraints for subdomain 2 are

$$W(x, \pm b/2) = \frac{\partial W(x, \pm b/2)}{\partial y} = 0. \tag{42}$$

The respective starting functions for each subdomain are thus given as follows:

$$\phi_1^{\{1\}}(x) = \phi_1^{\{2\}}(x) = x^2 - 0.25a^2, \tag{43a}$$

$$\psi_1^{\{1\}}(y) = y^2 - 0.25b^2, \tag{43b}$$

$$\psi_1^{\{2\}}(y) = (y + 0.5b)^2 (y - 0.5b)^2. \tag{43c}$$

Note that deflection functions for the simply-supported edge satisfy only the geometry requirement but not necessarily the natural boundary conditions.

3.2. *A simply-supported plate partially clamped along opposite centers*

The plate configuration for this case is shown in Fig. 3(b). Parts of the edges at $y = \pm b/2$ are clamped, thus the domain is divided along the clamped portions into three subdomains. Similar to the preceding case, the deflection functions in the x-direction are chosen to satisfy identically the simply-supported boundary conditions as in eqn (40). For subdomains 1 and 3, the edges at $y = \pm b/2$ are simply supported and the following boundary conditions apply:

$$W(x, \pm b/2) = \frac{\partial^2 W(x, \pm b/2)}{\partial y^2} = 0. \tag{44}$$

For subdomain 2, the clamped boundary conditions at $y = \pm b/2$ require

$$W(x, \pm b/2) = \frac{\partial W(x, \pm b/2)}{\partial y} = 0. \tag{45}$$

From the above boundary conditions, the basic functions assigned for each subdomain are:

$$\phi_1^{\{1\}}(x) = \phi_1^{\{2\}}(x) = \phi_1^{\{3\}}(x) = x^2 - 0.25a^2, \tag{46a}$$

$$\psi_1^{\{1\}}(y) = \psi_1^{\{3\}}(y) = y^2 - 0.25b^2, \tag{46b}$$

$$\psi_1^{\{2\}}(y) = (y + 0.5b)^2 (y - 0.5b)^2. \tag{46c}$$

3.3. *A simply-supported plate partially clamped from four corners*

For this case, the simply-supported plate is partially clamped symmetrically from the four corners. This domain is partitioned into nine subdomains as shown in Fig. 3(c). The deflection functions of each subdomain are constructed to satisfy the corresponding geometric boundary constraints at $x = \pm a/2$ and $y = \pm b/2$. For adjacent subdomains in the x-direction, the following boundary conditions apply:

$$W(\pm a/2, y) = \frac{\partial W(\pm a/2, y)}{\partial x} = 0, \quad \frac{b-c}{2} \leqslant |y| < b/2, \tag{47}$$

$$W(\pm a/2, y) = \frac{\partial^2 W(\pm a/2, y)}{\partial x^2} = 0, \quad 0 \leqslant |y| < \frac{b-c}{2}. \tag{48}$$

Similarly for adjacent subdomains in the y-direction, the applicable boundary constraints are

$$W(x, \pm b/2) = \frac{\partial W(x, \pm b/2)}{\partial y} = 0, \quad \frac{a-c}{2} \leqslant |x| < a/2, \tag{49}$$

$$W(x, \pm b/2) = \frac{\partial^2 W(x, \pm b/2)}{\partial y^2} = 0, \quad 0 \leqslant |x| < \frac{a-c}{2}. \tag{50}$$

The basic functions for each constitutive subdomain are therefore given as:

$$\phi^{\{\varepsilon\}}(x) = x^2 - 0.25a^2, \quad \varepsilon = \{1,4,8\}, \tag{51a}$$

$$\phi^{\{\varepsilon\}}(x) = (x+0.5a)^2(x-0.5a)^2, \quad \varepsilon = \{2,3,9\} \text{ and } \{5,6,7\}, \tag{51b}$$

$$\psi^{\{\varepsilon\}}(y) = y^2 - 0.25b^2, \quad \varepsilon = \{1,2,6\}, \tag{51c}$$

$$\psi^{\{\varepsilon\}}(y) = (y+0.5b)^2(y-0.5b)^2, \quad \varepsilon = \{3,4,5\} \text{ and } \{7,8,9\}. \tag{51d}$$

3.4. *A free plate partially supported from four corners*

The last case considered here, as shown in Fig. 3(d), involves free edges with partial simple supports. The method of partitioning is analogous to the preceding case. For this configuration, the related boundary conditions for the adjacent subdomains are:

$$W(\pm a/2, y) = \frac{\partial^2 W(\pm a/2, y)}{\partial x^2} = 0, \quad \frac{b-c}{2} \leqslant |y| < b/2, \tag{52}$$

$$\frac{\partial^2 W(\pm a/2, y)}{\partial x^2} = \frac{\partial^3 W(\pm a/2, y)}{\partial x^3} = 0, \quad 0 \leqslant |y| < \frac{b-c}{2}, \tag{53}$$

$$W(x, \pm b/2) = \frac{\partial^2 W(x, \pm b/2)}{\partial y^2} = 0, \quad \frac{a-c}{2} \leqslant |x| < a/2, \tag{54}$$

$$\frac{\partial^2 W(x, \pm b/2)}{\partial y^2} = \frac{\partial^3 W(x, \pm b/2)}{\partial y^3} = 0, \quad 0 \leqslant |x| < \frac{a-c}{2}. \tag{55}$$

The corresponding basic functions for each subdomain are:

$$\phi^{\{\varepsilon\}}(x) = 1, \quad \varepsilon = \{1,4,8\}, \tag{56a}$$

$$\phi^{\{\varepsilon\}}(x) = x - 0.25a^2, \quad \varepsilon = \{2,3,9\} \text{ and } \{5,6,7\}, \tag{56b}$$

$$\psi^{\{\varepsilon\}}(y) = 1, \quad \varepsilon = \{1,2,6\}, \tag{56c}$$

$$\psi^{\{\varepsilon\}}(y) = y - 0.25b^2, \quad \varepsilon = \{3,4,5\} \text{ and } \{7,8,9\}. \tag{56d}$$

4. RESULTS AND DISCUSSION

The vibratory characteristics of these plates are examined for isotropic and anisotropic materials respectively. Convergence tests and comparison studies are carried out to ascertain the validity of the proposed method for the solution of this class of problems.

Table 1. Convergence of frequency parameters, $\lambda = (\rho h\omega^2 a^4/D_0)^{1/2}$, for isotropic square plates with partial mixed discontinuous periphery boundaries as shown in Cases 1 to 4 ($\beta = 0.5$)

Case	No. of terms $I \times J$	Mode sequence number							
		1	2	3	4	5	6	7	8
1	10 × 10	25.67	52.11	59.97	88.14	100.6	112.2	135.1	145.2
	15 × 15	25.70	52.11	60.06	88.14	100.6	112.3	135.2	145.2
	16 × 16	25.70	52.11	60.08	88.13	100.6	112.3	135.2	145.2
	17 × 17	25.71	52.11	60.08	88.13	100.6	112.3	135.2	145.2
	18 × 18	25.71	52.11	60.08	88.13	100.6	112.3	135.2	145.2
2	10 × 10	28.31	53.20	67.45	89.58	100.2	125.5	134.0	144.6
	15 × 15	28.33	53.25	67.52	89.75	100.3	125.6	134.1	144.9
	16 × 16	28.33	53.26	67.54	89.76	100.4	125.7	134.1	144.9
	17 × 17	28.34	53.26	67.55	89.77	100.4	125.7	134.2	144.9
	18 × 18	28.34	53.26	67.56	89.77	100.4	125.7	134.2	144.9
3	10 × 10	25.23	57.39	57.39	96.60	101.0	112.9	147.4	147.4
	15 × 15	25.34	75.55	57.55	96.95	101.1	113.2	147.8	147.8
	17 × 17	25.38	57.60	57.60	97.00	101.1	113.3	147.8	147.8
	18 × 18	25.40	57.63	57.63	97.04	101.1	113.3	147.9	147.9
	19 × 19	25.40	57.63	57.63	97.05	101.1	113.3	147.9	147.9
4	10 × 10	18.12	42.51	42.51	63.00	75.63	78.12	92.63	92.63
	15 × 15	18.16	42.76	42.76	64.23	76.40	79.89	93.70	93.70
	16 × 16	18.20	42.95	42.95	64.85	76.42	80.60	94.58	94.58
	17 × 17	18.21	43.09	43.09	65.03	76.45	80.69	94.66	94.66
	18 × 18	18.21	43.10	43.10	65.03	76.46	80.70	94.66	94.66

4.1. *Convergence and comparison studies*

(a) *Isotropic plates.* To demonstrate the validity of the proposed method to the analysis of a mixed edge plate, convergence and comparison studies have been carried out for the isotropic mixed edge plates by setting $\nu_{12} = \nu_{21} = \nu = 0.3$, $D_{11} = D_{22} = D = Eh^3/[12(1-\nu^2)]$, and $D_{66} = 1/2[(1-\nu)D]$. The non-dimensional frequency parameters for the isotropic case is expressed as $\lambda = (\rho h\omega^2 a^4/D)^{1/2}$. Table 1 shows the convergence patterns of the frequency parameters with respect to the number of terms used in the admissible functions. The convergent results are compared in Table 2 with the established data obtained from the open literature.

For a simply-supported plate partially clamped along the end of two opposite edges (Case 1), frequency parameters obtained using the domain decomposition method are

Table 2. Comparison of frequency parameters, $\lambda = (\rho h\omega^2 a^4/D)^{1/2}$, for isotropic square plates with partial mixed discontinuous periphery boundaries $\beta = 0.5$ (Cases 1 to 4)

Case	Source of results	Mode sequence number					
		1	2	3	4	5	6
1	Ota and Hamada	25.5	—	—	—	—	—
	Fan and Cheung	26.37	52.23	61.78	—	—	—
	Present method	25.71	52.11	60.09	88.3	100.6	112.3
2	Ota and Hamada	28.3	—	—	—	—	—
	Keer and Stahl	28.37	—	—	—	—	—
	Narita	28.44	53.49	67.85	90.50	100.6	—
	Fan and Cheung	28.65	54.00	68.58	—	—	—
	Mizusawa and Leonard	28.63	53.84	68.40	91.60	101.0	—
	Present method	28.34	53.26	67.56	89.77	100.4	125.7
3	Narita	26.18	58.70	58.70	98.58	102.0	—
	Present method	25.40	57.63	57.63	97.05	101.1	113.3
4	Keer and Stahl	18.33	—	—	—	—	—
	Present method	18.21	43.10	43.10	65.03	76.46	80.70

compared with those derived from the analytical and numerical approaches reported in the literature. The fundamental frequency of 25.71 predicted in the present analysis is in very good agreement to the analytical results of 25.5 presented by Ota and Hamada (1963) whose formulation was based on the distributed moment function. The frequency parameters for higher modes are compared with the prediction of Fan and Cheung (1984) using the finite strip approximation. Close agreement is again observed in this case.

Several researchers have presented results for a simply-supported plate partially clamped along the center portion of two opposite edges (Case 2). Generally, it is observed that the computed natural frequencies of the present method are in closer agreement with those analytical results presented by Ota and Hamada (1963), Keer and Stahl (1972), and Narita (1981). The discretization methods (Venkateswara *et al.*, 1973; Fan and Cheung, 1984; Mizusawa and Leonard, 1990) seem to give a slightly higher estimate of the natural frequencies than those obtained by the present method and analytical methods.

Very limited data are available for the mixed edge plates considered in Cases 3 and 4. Narita (1981), has presented the frequency parameters for a simply-supported square plate partially clamped symmetrically from four corners (Case 3). The first five frequency parameters determined using the series type solution method and the present domain decomposition method are in close agreement. Keer and Stahl (1972) reported the fundamental frequency parameter of 18.33 for a free square plate simply-supported adjacent to four corners with $\beta = 0.5$ (Case 4). The predicted value of 18.23 by the domain decomposition approach again compared very well to the literature.

(b) *Anisotropic plates.* Unlike the isotropic plate, the vibrational response of plates with general anisotropy is affected by both the partial mixed ratio and the orientation of the fabric materials. The influence of partial mixed ratio and fiber orientation on the vibration frequency are examined. For this study, the plate is assumed to be made of Glass–epoxy material. The important mechanical properties of Glass–epoxy are: $E_1 = 138$ GPa, $E_2 = 8.96$ GPa, $G_{12} = 7.1$ GPa and $\nu_{12} = 0.30$.

The set of practical mixed edge plate configurations discussed earlier is now investigated for the anisotropic materials to demonstrate the dependence of the vibrational response on the fiber orientation. A convergence test is carried out to determine the number of terms required for satisfactory results. An anisotropic square plate with partial mixed ratio, $\beta = 0.5$ is considered. The computed frequencies are expressed in terms of non-dimensional parameters, $\lambda = (\rho h \omega^2 a^4/D_0)^{1/2}$, where $D_0 = E_1 h^3/[12(1-\nu_{12}\nu_{21})]$. The rates of convergence of the frequency parameters for the first eight modes of vibration are presented in Table 3.

In general, a monotonic upwards convergence for the frequency parameters is observed as the number of terms in the approximation increases. The fiber orientation has very little influence on the rate of convergence of the frequency parameters. For plates of more complex geometry, a higher number of terms is necessary to achieve a better convergence. For plates composed of two or three subdomains (Cases 1 and 2), the convergence is more rapid as compared to those having more subdomains (Cases 3 and 4).

From Table 3, it can be seen that the number of terms needed for a reasonable convergence of the frequency parameters for both Cases 1 and 2 (where three or less subdomains are involved) is 17×17 terms. For plates composed of more subdomains, a higher number of terms is required as it can be seen from Cases 3 and 4 (where nine subdomains are involved). They required 19×19 terms to achieve a reasonable convergence. In the present study, all the calculations performed in the numerical analysis are based on 19×19 terms.

4.2. *Numerical investigation and discussion*

To examine the combined effects of the partial mixed ratio β and fiber orientation θ on the vibrational behavior of fiber-reinforced anisotropic plates with mixed discontinuous periphery boundaries, various sets of data were computed for each plate configuration. Table 4 presents the frequency parameters of a simply-supported plate partially clamped along the end of two opposite edges (Case 1). The fiber orientation, θ, varies in the range 0–90°. The partial mixed ratio, β, takes on values of 0, 1/3, 1/2, 2/3 and 1. In the limiting

Table 3. Convergence of frequency parameters, $\lambda = (\rho h\omega^2 a^4/D_0)^{1/2}$, for anisotropic plates with partial mixed discontinuous edges, $\beta = 0.5$ and $\theta = 45°$

Case	No. of terms $I \times J$	Mode sequence number							
		1	2	3	4	5	6	7	8
1	10×10	20.31	40.49	48.12	70.21	80.60	88.25	101.4	117.6
	15×15	20.38	40.50	48.18	70.21	80.63	88.30	101.4	117.9
	16×16	20.40	40.50	48.20	70.21	80.64	88.34	101.4	117.9
	17×17	20.41	40.51	48.21	70.21	80.64	88.35	101.4	117.9
	18×18	20.41	40.51	48.21	67.21	80.64	88.35	101.4	117.9
2	10×10	22.23	41.62	52.73	67.37	80.20	97.15	101.7	118.1
	15×15	22.26	41.65	52.77	67.40	80.24	97.17	101.9	118.4
	16×16	22.26	41.66	52.79	67.41	80.24	97.18	101.9	118.4
	17×17	22.26	41.68	52.79	67.47	80.25	97.20	101.9	118.4
	18×18	22.26	41.68	52.79	67.41	80.25	97.20	101.9	118.4
3	10×10	20.60	40.45	51.24	70.10	79.33	96.10	106.2	115.6
	15×15	20.69	40.55	51.27	70.35	79.38	96.34	106.8	115.9
	16×16	20.70	40.57	51.31	70.38	79.40	96.38	107.0	115.9
	17×17	20.72	40.60	51.33	70.40	79.41	96.47	107.1	115.9
	18×18	20.73	40.62	51.36	70.41	79.42	96.50	107.1	115.9
	19×19	20.73	40.62	51.36	70.42	79.42	96.50	107.1	115.9
4	10×10	14.61	30.63	37.59	50.43	53.92	67.27	72.94	80.93
	15×15	14.64	30.67	37.67	50.47	54.05	67.35	73.04	81.13
	16×16	14.65	30.69	37.73	50.49	54.10	67.37	73.09	81.20
	17×17	14.66	30.72	37.77	50.51	54.14	67.42	73.12	81.26
	18×18	14.67	30.72	37.79	50.52	54.15	67.44	73.15	81.34
	19×19	14.67	30.72	37.79	50.52	54.16	67.46	73.16	81.36

Table 4. Frequency parameters, $\lambda = (\rho h\omega^2 a^4/D_0)^{1/2}$, for simply-supported anisotropic square plates partially clamped along the ends of two opposite edges (Case 1)

β	θ	Mode sequence number							
		1	2	3	4	5	6	7	8
0.0	0°	15.19	33.30	44.42	60.78	64.53	90.30	93.66	108.6
	30°	15.80	35.58	42.53	60.77	71.60	85.59	92.58	108.5
	45°	16.00	36.50	41.75	60.97	76.67	80.02	93.11	108.4
	60°	15.80	35.58	42.53	60.77	71.60	85.59	92.58	108.5
	90°	15.19	33.30	44.42	60.78	64.53	90.30	93.66	108.6
1/3	0°	17.05	36.79	45.56	65.09	68.84	93.59	98.87	110.1
	30°	17.85	38.55	44.69	64.88	76.40	86.59	99.45	110.8
	45°	18.35	38.63	45.49	65.59	77.95	85.43	99.33	112.7
	60°	18.47	37.80	46.95	66.44	73.10	91.19	98.41	115.6
	90°	18.15	36.71	48.17	65.93	69.79	95.87	97.63	109.7
1/2	0°	18.74	40.66	45.64	65.52	74.22	94.45	100.0	112.2
	30°	19.65	41.66	45.74	66.42	81.27	86.93	100.9	115.1
	45°	20.41	40.51	48.21	67.21	80.64	88.35	101.4	117.9
	60°	21.00	38.94	50.94	67.80	75.58	94.39	102.4	120.0
	90°	21.34	37.14	53.13	67.03	72.96	98.56	103.1	110.1
2/3	0°	19.97	44.24	46.28	66.91	80.56	94.62	101.5	112.6
	30°	21.02	43.29	48.58	68.30	86.82	87.97	102.2	116.5
	45°	22.10	41.68	52.29	69.11	81.20	95.74	102.0	120.6
	60°	23.20	40.02	56.49	68.98	76.61	100.5	105.9	121.1
	90°	24.40	38.00	60.91	67.35	73.56	100.4	109.0	115.2
1.0	0°	20.43	45.68	47.03	69.52	83.71	95.28	106.2	115.2
	30°	21.63	43.95	50.63	70.74	87.73	91.88	105.7	120.0
	45°	22.91	42.61	54.88	71.54	82.63	101.1	105.2	124.4
	60°	24.24	41.38	59.78	71.14	79.48	104.7	112.1	121.6
	90°	25.62	39.94	65.42	68.82	78.58	104.4	111.6	124.9

Table 5. Frequency parameters, $\lambda = (\rho h\omega^2 a^4/D_0)^{1/2}$, for simply-supported anisotropic square plates partially clamped at the center of two opposite edges (Case 2)

		Mode sequence number							
β	θ	0.0	2	3	4	5	6	7	8
0.0	0°	15.19	33.30	44.42	60.78	64.53	90.30	93.66	108.6
	30°	15.80	35.58	42.53	60.77	71.60	85.59	92.58	108.5
	45°	16.00	36.50	41.75	60.97	76.67	80.02	93.11	108.4
	60°	15.80	35.58	42.53	60.77	71.60	85.59	92.58	108.5
	90°	15.19	33.30	44.42	60.78	64.53	90.30	93.66	108.6
1/3	0°	19.54	43.06	45.53	64.21	78.34	94.52	95.80	109.8
	30°	20.45	42.61	46.91	65.68	83.87	87.55	98.05	112.3
	45°	21.37	40.68	50.35	66.33	79.50	93.07	97.94	115.2
	60°	22.32	38.54	54.39	66.04	73.69	96.88	102.3	117.1
	90°	23.44	35.90	59.14	65.81	66.75	95.67	108.8	112.7
1/2	0°	20.11	44.72	46.36	67.02	81.67	94.65	101.0	111.9
	30°	21.15	43.39	48.93	68.47	86.45	88.91	102.5	114.6
	45°	22.26	41.68	52.79	69.41	80.25	97.20	101.9	118.4
	60°	23.44	39.99	57.39	69.31	75.22	100.4	107.5	120.2
	90°	24.82	38.03	63.00	66.72	72.52	97.48	109.4	119.6
2/3	0°	20.36	45.46	46.86	68.86	83.27	95.03	104.8	114.1
	30°	21.50	43.80	50.12	70.16	87.36	90.78	105.1	117.9
	45°	22.72	42.32	54.24	71.09	81.53	99.85	104.4	122.4
	60°	24.02	40.96	59.10	70.80	77.76	103.5	110.8	121.1
	90°	25.45	39.44	64.91	68.09	76.94	101.7	110.7	123.8
1.0	0°	20.43	45.68	47.03	69.52	83.71	95.28	106.2	115.2
	30°	21.63	43.95	50.63	70.74	87.73	91.88	105.7	120.0
	45°	22.91	42.61	54.88	71.54	82.63	101.1	105.2	124.4
	60°	24.24	41.38	59.78	71.14	79.48	104.7	112.1	121.6
	90°	25.62	39.94	65.42	68.82	78.58	104.4	111.6	124.9

case where $\beta = 0.0$ or 1.0, the frequencies obtained are identical to that of a S-S-S-S square plate or a S-C-S-C square plate, respectively. It is observed that an increase in the partial clamped ratio raised the frequency of vibration at all fiber orientation angles. It is also noted that for a S-S-S-S plate (limiting case of $\beta = 0.0$), the frequency parameters increase to a peak at fiber orientation of 45°, and then decrease in a symmetric manner. The presence of the partial clamped ratio also affects the vibrational response. It depends on the extent of the partial clamping imposed, the peak fundamental frequency gradually shifts away from occurring at the fiber angle of 45° to higher fiber orientation angle.

The displacement contour plots to represent the mode shapes of the anisotropic plate with partial clamped ratio of 0.5 are presented in Fig. 4. For the mode of vibration anti-symmetry about the y-axis, the natural frequency increases from 40.66 to 53.13 as the fiber orientation, θ, changes from 0 to 90°. On the other hand, for mode of vibration anti-symmetry about the x-axis, the natural frequency reduces from 45.64 to 37.14 as the fiber orientation angle increases. Moreover mode switching has occurred which can be seen from the contour plots.

Similar phenomena are found for the case of a simply-supported plate partially clamped along the center of two opposite edges (Case 2). In Table 5, the variation of frequency parameters is presented with respect to fiber orientation and partial clamped ratios. The displacement contour plots of the mode shapes for the anisotropic plate with partial mixed ratio, $\beta = 0.5$ are presented in Fig. 5. Again mode switching is evident as the fiber angle varies.

For Cases 3 and 4, the plates are partially mixed in a symmetric manner, thus the effect of varying fiber orientation on the vibration behavior will be symmetrical about $\theta = 45°$. The frequency parameters are found to increase with respect to both the partial support ratio and the fiber orientation angle within the range of 0–45°. Table 6 presents the frequency parameters for the simply-supported anisotropic plate partially clamped symmetrically from the four corners (Case 3). The corresponding contour plots of the mode shapes for

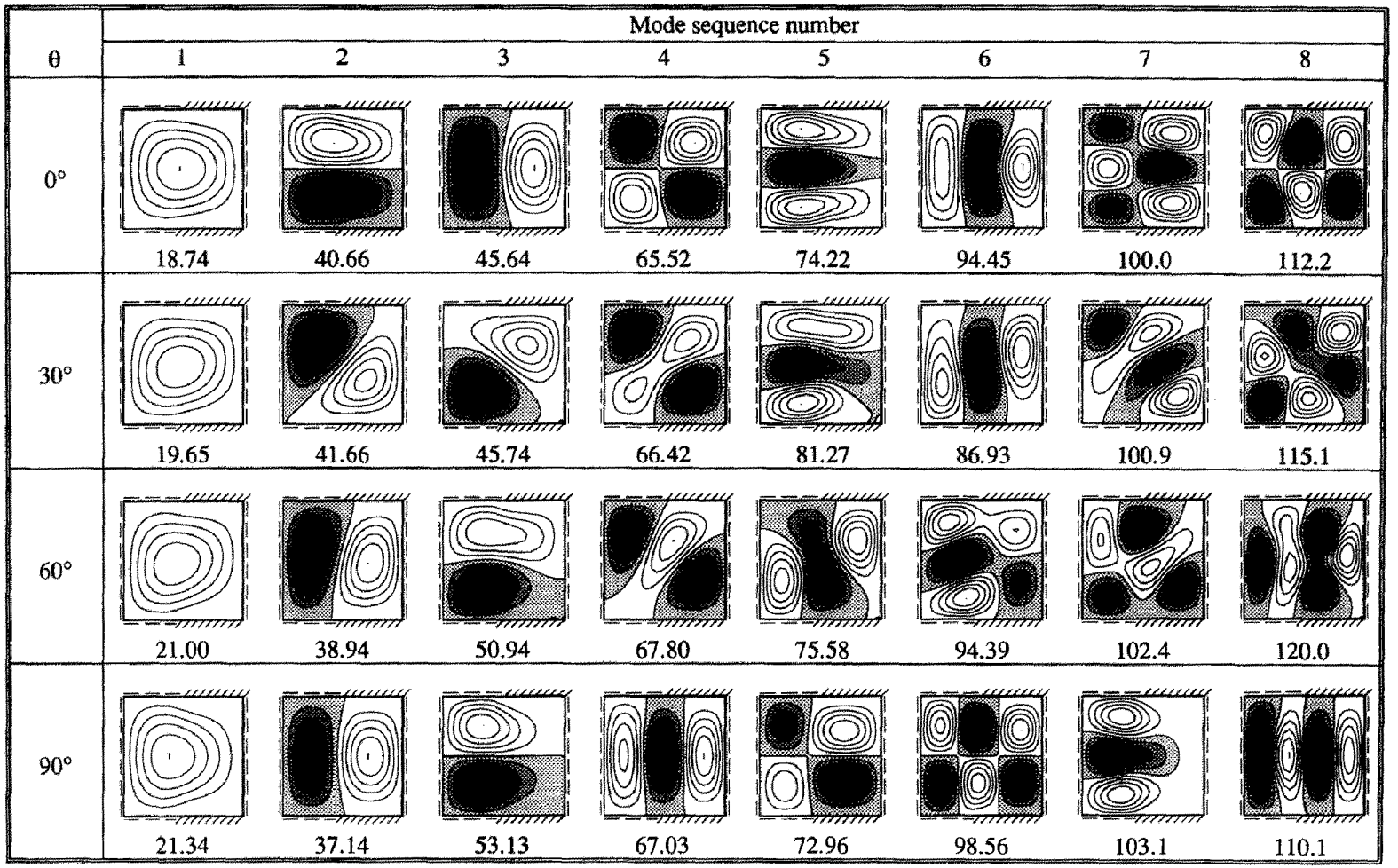

Fig. 4. Contour plots of deflection mode shapes for the simply-supported square anisotropic plate partially clamped ($\beta = 0.5$) along the ends of two opposite edges (Case 1).

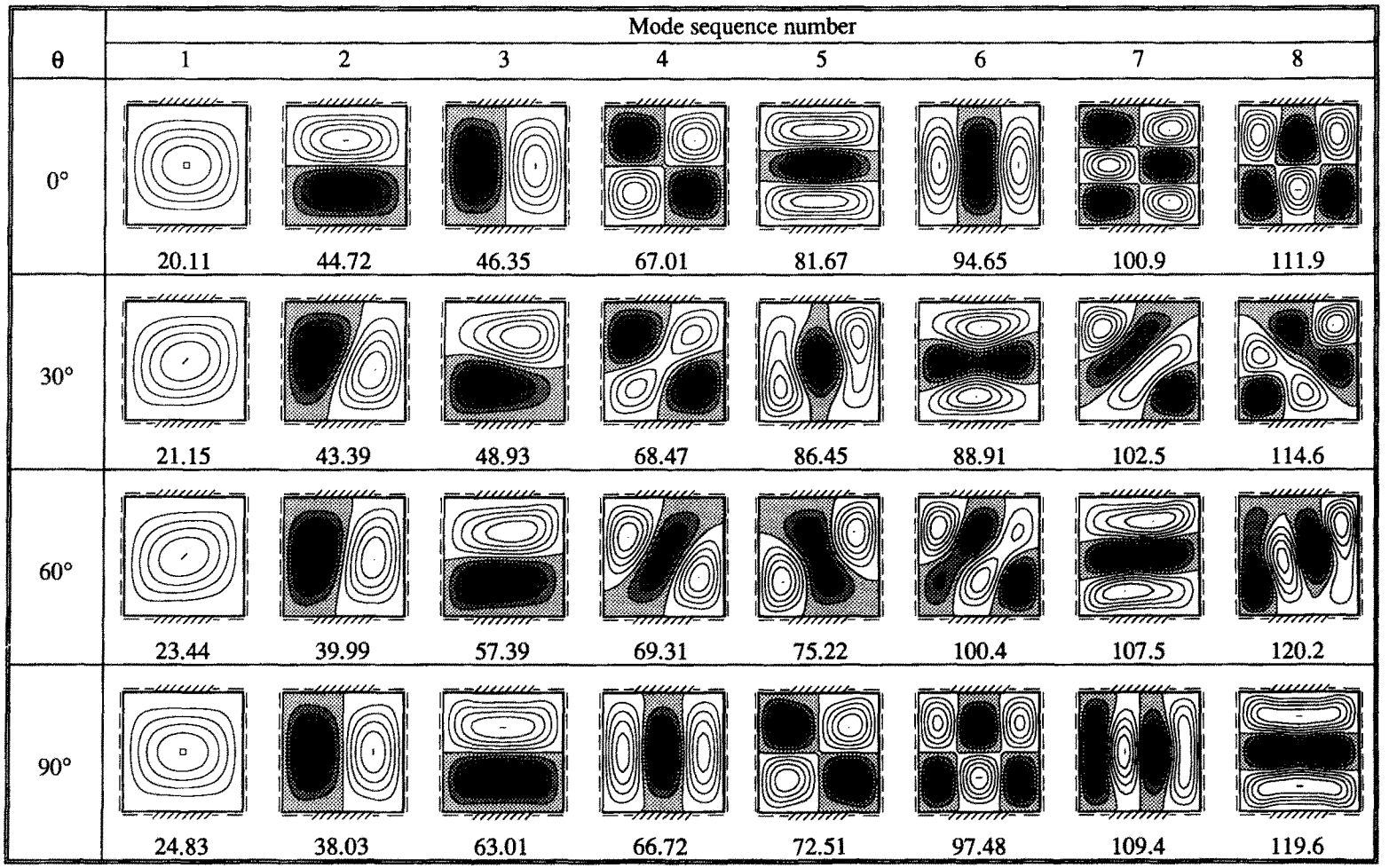

Fig. 5. Contour plots of deflection mode shapes for the simply-supported square anisotropic plate partially clamped ($\beta = 0.5$) at the center of two opposite edges (Case 2).

Table 6. Frequency parameters, $\lambda = (\rho h\omega^2 a^4/D_0)^{1/2}$, for simply-supported anisotropic square plates partially clamped symmetrically from the four corners (Case 3)

		Mode sequence number							
β	θ	1	2	3	4	5	6	7	8
0.0	0°	15.19	33.30	44.42	60.78	64.53	90.30	93.66	108.6
	15°	15.39	34.01	43.83	60.60	66.67	91.19	91.35	108.8
	30°	15.80	35.58	42.53	60.77	71.60	85.59	92.58	108.5
	45°	16.00	36.50	41.75	60.97	76.67	80.02	93.11	108.4
1/3	0°	17.21	36.72	47.03	67.71	68.10	96.48	100.1	109.2
	15°	17.47	37.04	46.99	66.02	71.21	94.97	99.65	110.5
	30°	18.00	37.63	46.95	65.39	75.03	91.59	99.09	112.9
	45°	18.26	37.90	46.96	65.29	77.13	89.50	98.88	113.9
1/2	0°	19.84	40.56	50.51	70.76	75.81	100.6	107.8	112.3
	15°	20.07	40.53	50.79	70.91	76.20	99.90	107.4	113.8
	30°	20.52	40.56	51.21	70.70	77.97	97.93	107.1	115.7
	45°	20.73	40.62	51.36	70.42	79.42	96.50	107.1	115.9
2/3	0°	23.49	45.08	56.13	75.82	82.68	107.7	112.7	119.0
	15°	23.60	45.03	56.21	76.58	82.00	107.0	112.8	122.0
	30°	23.80	45.14	56.09	76.67	83.32	104.3	114.0	122.1
	45°	23.90	45.28	55.89	76.13	85.48	101.9	115.6	119.5
1.0	0°	29.10	50.83	67.29	85.68	87.14	118.6	126.1	136.9
	15°	28.89	51.38	65.90	84.29	89.83	118.9	122.7	139.2
	30°	28.48	52.93	62.68	83.23	95.21	114.1	119.6	138.2
	45°	28.27	54.25	60.53	82.90	101.7	105.8	119.9	136.9

Table 7. Frequency parameters, $\lambda = (\rho h\omega^2 a^4/D_0)^{1/2}$, for completely free anisotropic square plates partially supported symmetrically from the four corners (Case 4)

		Mode sequence number							
β	θ	1	2	3	4	5	6	7	8
0.0	0°	10.03	14.13	22.38	24.74	29.92	39.41	48.70	49.39
	15°	10.22	14.18	21.75	24.75	30.26	39.97	47.62	51.49
	30°	10.63	14.38	20.37	24.89	30.60	42.38	47.26	53.39
	45°	10.86	14.59	19.56	25.03	30.58	46.14	47.28	48.59
1/3	0°	12.01	25.71	26.40	36.50	47.96	52.73	59.12	65.78
	15°	12.15	24.93	27.73	36.17	46.25	55.90	58.11	66.27
	30°	12.42	24.28	29.54	35.48	45.00	56.42	60.15	66.60
	45°	12.56	24.02	30.39	35.15	44.75	55.68	61.92	66.51
1/2	0°	13.99	30.78	35.26	49.88	58.86	61.84	71.99	76.79
	15°	14.16	30.86	35.78	49.95	56.25	66.07	70.66	78.31
	30°	14.50	30.82	37.06	50.26	54.57	68.51	71.07	80.52
	45°	14.67	30.72	37.79	50.52	54.16	67.46	73.16	81.36
2/3	0°	14.95	32.79	42.57	60.52	61.67	84.00	85.41	100.3
	15°	15.15	33.40	42.19	59.80	63.68	83.38	86.62	100.4
	30°	15.53	34.62	41.44	59.71	67.03	81.25	89.30	97.21
	45°	15.73	35.22	41.08	59.85	69.20	79.38	92.02	93.68
1.0	0°	15.19	33.30	44.42	60.78	64.53	90.30	93.66	108.6
	15°	15.39	34.01	43.83	60.60	66.67	91.19	91.35	108.8
	30°	15.80	35.58	42.53	60.77	71.60	85.59	92.58	108.5
	45°	16.00	36.50	41.75	60.97	76.67	80.02	93.11	108.4

partial mixed ratio of 0.5 are depicted in Fig. 6. For Case 4, the frequency parameters are presented in Table 7. The corresponding contour plots at each orientation angle are given in Fig. 7.

5. CONCLUSIONS

This paper presents the detailed formulation of the domain decomposition method for vibration analysis of anisotropic square plates with different combinations of mixed edge

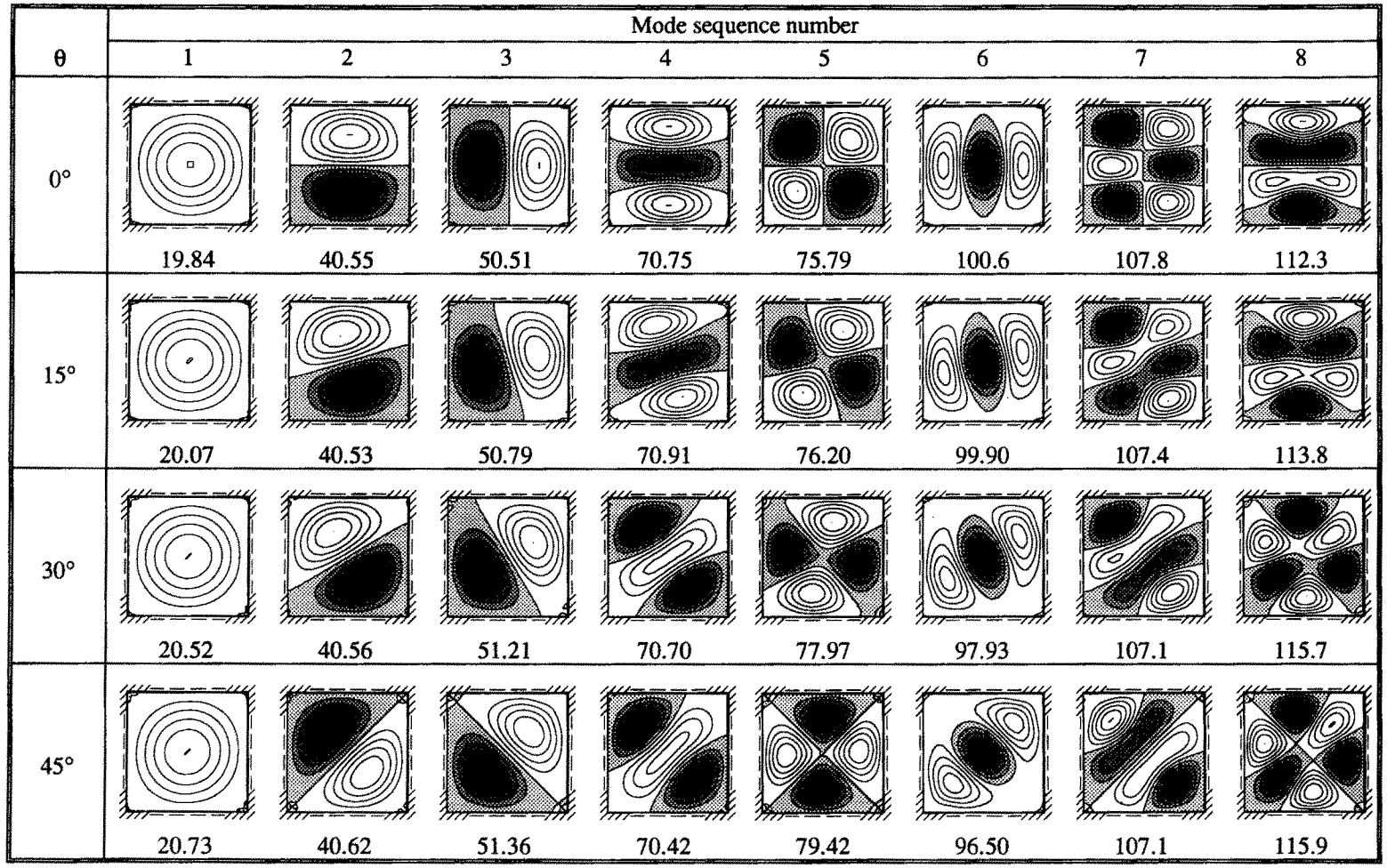

Fig. 6. Contour plots of deflection mode shapes for the simply-supported square anisotropic plate partially clamped ($\beta = 0.5$) symmetrically from the four corners (Case 3).

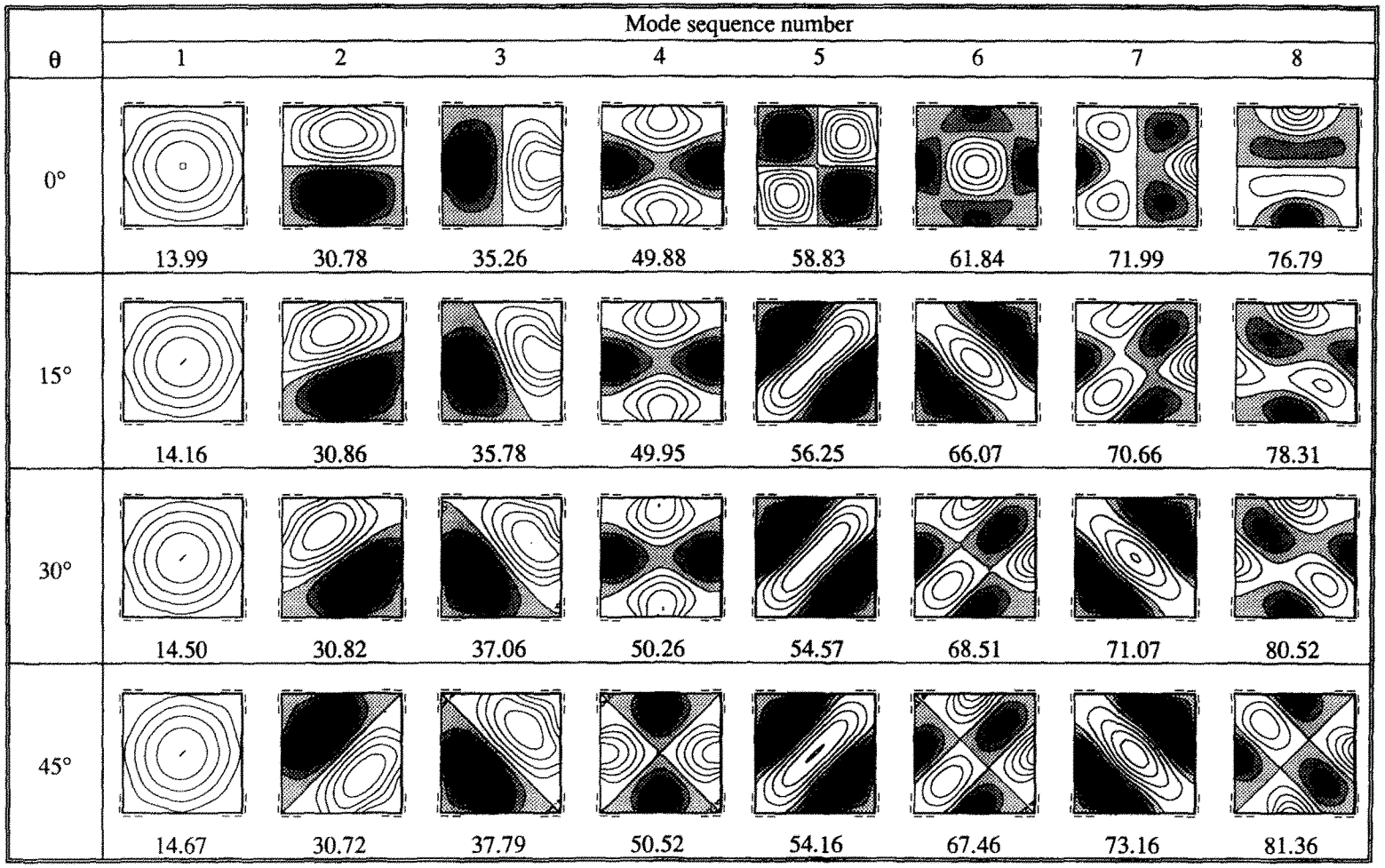

Fig. 7. Contour plots of deflection mode shapes for the completely free square anisotropic plate partially supported ($\beta = 0.5$) symmetrically from the four corners (Case 4).

boundary conditions. The flexibility and accuracy of the method have been demonstrated. The important merit of the method lies in its computational efficiency. Regardless of the number of subdomains involved, the assembling process of the global stiffness and mass matrices is such that the size of the final eigenvalue equation is kept small. Consequently, the computational time and storage space will not increase substantially as the problem size increases.

It is evident that the proposed method can be easily extended to a wider class of plate problems which cannot be solved in the direct use of the traditional Rayleigh–Ritz approach. The present method has been applied to investigate several anisotropic square plates with mixed discontinuous periphery boundaries. To validate the accuracy of the method, the frequency parameters obtained for the isotropic case are compared with the established analytical and numerical results in the open literature. Excellent agreement was found in all cases considered. An investigation into the effects of varying fiber orientation angle and partial mixed ratio on the frequency parameters of these square plates has been discussed. Frequency parameters computed were presented in tabulated form and the deflection mode shapes in the form of contour plots have also been presented to further enhance our understanding of the vibratory characteristics of anisotropic plates with partial mixed periphery boundaries.

REFERENCES

Ashton, J. E. (1969). Natural modes of free-free anisotropic plates. *Shock Vibr. Bull.* **39,** 93–100.

Bert, C. W. (1977a). Fundamental frequency of orthotropic plates with various planforms and edge conditions. *Shock Vibr. Bull.* **47,** 89–94.

Bert, C. W. (1977b). Optimal design of a composite-material plate to maximize its fundamental frequency. *J. Sound Vibr.* **50,** 229–237.

Chelladurai, T., Shastry, B. P. and Rao, G. V. (1984). Effect of fiber orientation on the vibration behavior of orthotropic rectangular plates. *Fibre Sci. Technol.* **21,** 73–81.

Chihara, T. S. (1978). *An Introduction to Orthogonal Polynomials.* Gordon and Breach, New York.

Fan, S. C. and Cheung, Y. K. (1984). Flexural free vibrations of rectangular plates with complex support conditions. *J. Sound Vibr.* **93,** 81–94.

Gorman, D. J. (1984). An exact analytical approach to the free vibration analysis of rectangular plates with mixed boundary conditions. *J. Sound Vibr.* **93,** 235–247.

Grandin, H., Jr (1986). *Fundamentals of The Finite Element Method.* Macmillan, New York.

Keer, L. M. and Stahl, B. (1972). Eigenvalue problems of rectangular plates with mixed edge conditions. *ASME J. Appl. Mech.* **39,** 513–520.

Liew, K. M., Hung, K. C. and Lam, K. Y. (1993a). On the use of substructure methods for vibration analysis of rectangular plates with discontinuous boundary conditions. *J. Sound Vibr.* **163,** 451–462.

Liew, K. M., Hung, K. C. and Lim, M. K. (1993b). Roles of domain decomposition method in plate vibrations: treatment of mixed discontinuous periphery boundaries. *Int. J. Mech. Sci.* **35,** 615–632.

Liew, K. M., Lam, K. Y. and Chow, S. T. (1989). Study on flexural vibration of triangular composite plates influenced by fiber orientation. *Compos. Struct.* **13,** 123–132.

Malhotra, S. K., Genesan, N. and Veluswami, M. A. (1988). Effect of fiber orientation and boundary conditions on the vibration behavior of orthotropic square plates. *Compos. Struct.* **9,** 247–255.

Mizusawa, T. and Leonard, J. W. (1990). Vibration and buckling of plates with mixed boundary conditions. *Engng Struct.* **12,** 285–290.

Mohan, D. and Kingsbury, H. D. (1971). Free vibration of generally orthotropic plates. *J. Acoust. Soc. Am.* **55,** 998–1002.

Narita, Y. (1981). Application of a series-type method to vibration of orthotropic rectangular plates with mixed boundary conditions. *J. Sound Vibr.* **77,** 345–355.

Ota, T. and Hamada, M. (1963). Fundamental frequencies of simply supported but partially clamped square plates. *Bull. Japan Soc. Mech. Engrs* **6,** 397–403.

Venkateswara, R., Raju, G. and Murthy, T. V. (1973). Vibration of rectangular plates with mixed boundary conditions. *J. Sound Vibr.* **30,** 257–260.

Vinson, J. R. and Sierakowski, L. (1986). *The Behavior of Structures Composed of Composite Materials.* Martinus Nijhoff, Dordrecht, Netherlands.

Whitney, J. M. (1971). Free vibration of anisotropic rectangular plates. *J. Acoust. Soc. Am.* **52,** 448–449.

Yuan, J. and Dickinson, S. M. (1992). The flexural vibration of rectangular plate systems approached by using artificial springs in the Rayleigh–Ritz method. *J. Sound Vibr.* **159,** 39–55.